STREAMFLOW CHANGES IN THE SIERRA NEVADA, CALIFORNIA, SIMULATED USING A STATISTICALLY DOWNSCALED GENERAL CIRCULATION MODEL SCENARIO OF CLIMATE CHANGE[*]

ROBERT L. WILBY
Division of Geography
University of Derby, Kedleston Road, Derby, DE22 1GB, UK
@National Center for Atmospheric Research
Boulder, Colorado, 80307-3000, USA

MICHAEL D. DETTINGER
U.S. Geological Survey
Water Resources Division, California District
Scripps Institution of Oceanography
9500 Gilman Drive, La Jolla, California, 92093-0224

1. Introduction

Simulations of future climate using general circulation models (GCMs) suggest that rising concentrations of greenhouse gases may have significant consequences for the global climate. Of less certainty is the extent to which regional scale (i.e., sub-GCM grid) environmental processes will be affected. This is because the length scales of GCMs (which are typically about 200 kilometres) are too coarse to resolve complex orography and important sub-grid scale processes such as convective precipitation. Furthermore, GCM output representing the surface climate under current conditions is commonly unreliable at the scale of individual grid points (see Table 1 below). Ironically, these are the scales that are likely to be of greatest interest to resource managers who have functional responsibilities that cover relatively small geographical areas. In other words, there is a scale mismatch between the scale of global change scenarios and the data requirements of the impacts analyst (Hostetler, 1994). "Downscaling" techniques have subsequently emerged as a means of bridging the gap between what climatologists currently are able to supply and what regional climate-change impact studies require.

In this chapter, a range of downscaling techniques are critiqued. Then a relatively simple (yet robust) statistical downscaling technique and its use in the modelling of future runoff scenarios for three river basins in the Sierra Nevada, California, is described. This region was selected because GCM experiments driven by combined greenhouse-gas and sulphate-aerosol forcings consistently show major changes in the hydroclimate of the southwest United States by the end of the 21st century. Shown in

---

[*] *Chapter 6 in "Linking Climate Change to Land Surface Change," 2000, S. McLaren and D. Kniveton (eds.), Kluwer Academic Publishers, Netherlands.*

Figure 1, for example, are projected changes in winter (DJF) precipitation from the Canadian Centre for Climate Modelling and Analysis (CGCM1) and by the U.K. Meteorological Office's Hadley Centre for Climate Prediction and Research (HadCM2) transient climate-change simulations (Flato et al., 1999; Boer et al., 1999a,b; Johns et al., 1997; Mitchell and Johns, 1997). Both experiments have been central to the U.S. National Assessment of the Potential Consequences of Climate Variability and Change (see http://www.nacc.usgcrp.gov/), and both predict increases in winter precipitation over California by 2090-99.
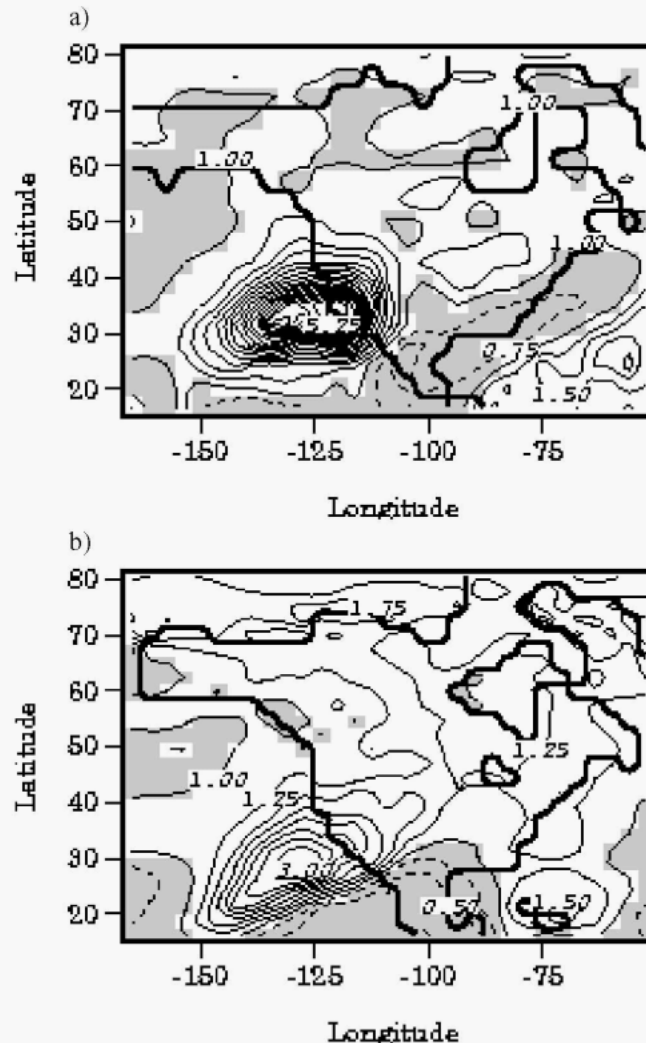

FIGURE 1. Precipitation ratios over North America (future [2090-99]/ current [1961-90]) for December, January, and February projected by a) CGCM1, b) HadCM2 (Felzer, 1999). Shading indicates grid boxes where the ratio is less than 1.0.

Although the scenarios in Figure 1 (along with accompanying temperature increases) imply major changes in regional snowpack, snowmelt, and runoff, confidence in HadCM2 scenarios at the basin scale is low. For example, Table 1 shows significant differences between observed and HadCM2-derived precipitation statistics for the heterogeneous landscape of the San Juan basin, Colorado. This deficiency is addressed herein by exploiting observed correlations between climate variables at the GCM grid-scale (such as geopotential height fields) and daily weather at the station scale (such as single-site precipitation). These empirical relationships are used to project future changes in atmospheric circulation and humidity in the HadCM2 climate-change scenarios to the station scale. A hydrological model is then used to simulate streamflows in each basin under the downscaled current- and future-climate conditions.

TABLE 1. A comparison of observed and HadCM2 daily precipitation for the San Juan River basin, Colorado. The observed data were derived from 37 stations for the period 1979-95 with mean elevation 2600 m. The HadCM2 data were obtained from the nearest grid point, which has a resolution of 2.5° latitude by 3.75° longitude and elevation 1900 m.

	Daily precipitation diagnostics (mm)				
	Mean	Standard Deviation	90%	%Wet	Annual
Observed	4.6	5.8	11.8	53.0	891
GCM	1.6	2.0	4.2	78.4	450

2. Downscaling Techniques

The theory and practice of downscaling has been reviewed elsewhere (see Giorgi and Mearns, 1991; Wilby and Wigley, 1997; Wilby et al., 1998b). Therefore, we provide only a brief overview of the main downscaling approaches, namely (a) dynamical, (b) weather typing, (c) stochastic, and (d) regression-based methods.

2.1 DYNAMICAL

Dynamical downscaling includes the nesting of a high-resolution regional climate model (RCM) within a GCM (Christensen et al., 1997; McGregor, 1997). The RCM uses the GCM to define time-varying atmospheric boundary conditions around a finite domain, within which the physical dynamics of the atmosphere are modelled using horizontal grid spacings of 20-50 km. The main limitation of RCMs is that they are as computationally demanding as GCMs (placing constraints on the domain size, number of experiments, and duration of simulations). However, RCMs can better resolve smaller scale atmospheric features, such as orographic precipitation, than the host GCM (Jones et al., 1995) and are able to respond in physically consistent ways to different external forcings such as land-surface or atmospheric-chemistry changes (Giorgi and Mearns, 1999).

2.2 WEATHER TYPING

Weather-typing approaches involve the stratification of local meteorological variations by concomitant, synoptic-scale (1000 km) atmospheric circulation patterns (e.g., Hay et al., 1992; Matyasovsky et al., 1994). Future regional climate scenarios are then constructed by resampling observed variables from probability distributions conditioned on synthetic series of circulation patterns (e.g., Bardossy and Plate, 1992; Dettinger and Cayan, 1992; Goodess and Palutikof, 1998). The main appeal of circulation-based downscaling is that it is founded on sensible linkages between climate on the large scale, which GCMs are best suited to project, and weather at the local scale. The technique is also readily applicable to a wide variety of environmental variables and can preserve some of the spatial auto-correlation between multiple sites and multiple variables (e.g., precipitation and temperature). However, weather-typing schemes commonly are parochial, have difficulty simulating extreme events, and must assume stationary circulation-to-surface climate conditioning (Wilby, 1997). Precipitation scenarios produced by circulation changes alone are also relatively insensitive to future climate forcing (see Wilby et al., 1998b).

2.3 STOCHASTIC

The most popular stochastic downscaling approach involves modifying parameters in conventional weather generators such as Richardson's (1981) Weather-GENeration program (WGEN). The standard WGEN program simulates precipitation occurrence using a two-state, first-order Markov chain; precipitation amounts on wet days using a gamma distribution; and temperature and radiation components using first-order trivariate autoregression that is conditional on precipitation occurrence. Future-climate scenarios are generated stochastically using revised parameter sets that have been scaled in direct proportion to the corresponding variable changes in a GCM (Wilks, 1992). The main advantage of the technique is that it can exactly reproduce key climate statistics and has been widely used for climate-impact assessment (e.g., Mearns et al., 1996). The key disadvantages relate to the arbitrary manner in which model parameters are changed for future-climate conditions, to the unanticipated effects that these changes can have on conditional variables (Katz, 1996), and to the poor representation of interannual variability in stochastic models (Gregory et al., 1993).

2.4 REGRESSION

Regression-based downscaling methods employ empirical relationships between local scale/single-site predictand(s) and synoptic-scale predictor(s). Techniques differ according to the choice of mathematical transfer function, predictor variable suite, or statistical-fitting procedure. Methods include linear and non-linear regression, artificial neural networks, canonical correlation, and principal components analyses (e.g., Conway et al., 1996; Crane and Hewitson, 1998; von Storch et al., 1993). The main strengths of regression downscaling are the relative ease of application and the parsimony of the models. However, regression models typically explain only a fraction of the observed climate variability. In common with weather-typing methods, stationarity of the empirical

relationships is also assumed, and downscaled scenarios can be sensitive to the choice of predictor variables and regression method (Winkler et al., 1997). Still, regression models provide an efficient compromise between simpler, purely stochastic weather generators and computationally expensive, dynamical models. Regressions are inexpensive to apply but are able to reproduce physically realistic intervariable, temporal, and spatial relationships as well as sequences in predicted fields that are present in historical records.

3. Data and Modelling Methods

In light of these considerations, a regression-based statistical-downscaling model was applied to generate climatic inputs for streamflow simulations of current- and future-climate scenarios. Two sets of GCM output were used: the first to calibrate and then verify the coupled downscaling-hydrological model, and the second to downscale GCM output in order to simulate future streamflow in the Sierra Nevada.

3.1. PREDICTOR VARIABLES

Table 2 lists 15 candidate variables that were originally selected by Wilby et al. (1999) for possible use as downscaling predictors. All variables were derived from combinations of daily grid-point estimates of mean sea level pressure (mslp); 500 hPa geopotential height (H); 2-metre (near-surface) temperature (T2m); and 0.995-sigma-level (near-surface) relative humidity (RH), obtained from the National Center for Environmental Prediction / National Center for Atmospheric Research (NCEP/NCAR) Reanalysis (referred to hereafter as Reanalysis; Kalnay et al., 1996) of atmospheric observations for the period 1979 to 1995. The Reanalysis estimates were re-gridded from the NCEP grid (1.875° of latitude by 1.875° of longitude) to the 2.5° of latitude by 3.75° of longitude grid on which climate variations are represented in the HadCM2 simulations. The pressure data were used to calculate five daily airflow indices (U, V, F, Z, D) for both the surface (s) and the 500-mb level in the upper (u) atmosphere, according to a methodology described by Jones et al. (1993). Daily mean temperatures and relative humidities were used to estimate daily mean specific humidities (SH) by Richards' (1971) non-linear approximation.

The GCM used to drive the downscaling model in climate-change experiments was the U.K. Meteorological Office Hadley Centre's coupled ocean/atmosphere model (HadCM2) forced by combined CO_2 and albedo (as a proxy for sulphate aerosol) changes (Johns et al., 1997; Mitchell and Johns, 1997). In this sulphate-plus-greenhouse gas experiment (their "SUL" experiment), the model run begins in 1861 and is forced with an estimate of historical radiative conditions to 1993 followed by a projected future-forcing scenario with 1% increases in CO_2 and sulphate per year from 1994 to 2100. HadCM2 output for the period 1980-99 was used as a proxy for the current climate (as in previous downscaling studies, such as Conway et al., 1996; Pilling et al., 1998; Wilby et al., 1998a,b). Output for 2080 to 2099 was used to downscale climate conditions arising from future anthropogenic emissions of greenhouse gases and aerosols.

TABLE 2. Candidate predictor variables for downscaling HadCM2 daily output

Predictor Variable	Abbrev.	Source
Surface Variables (sea level)		
Mean sea level pressure	mslp	NCEP/NCAR
Zonal velocity component	Us	derived from mslp
Meridional velocity component	Vs	derived from mslp
Strength of the resultant flow (hPa)	Fs	derived from mslp
Vorticity (hPa)	Zs	derived from mslp
Divergence (hPa)	Ds	derived from mslp
2 meter temperatures (˚C)	T2m	NCEP/NCAR
Relative humidities (%)	RH	NCEP/NCAR
Specific humidity (gm/kg)	SH	derived from RH and T2m
Upper-atmosphere variables (500 hPa)		
500 hPa geopotential heights (m)	H	NCEP/NCAR
Zonal velocity component	Uu	derived from H
Meridional velocity component	Vu	derived from H
Strength of the resultant flow (hPa)	Fu	derived from H
Vorticity (hPa)	Zu	derived from H
Divergence (hPa)	Du	derived from H

3.2. STATISTICAL DOWNSCALING MODEL

The statistical downscaling model (Wilby et al., 1999) was calibrated by regressions linking selected Reanalysis grid-point values as independent predictor variables with daily weather data for seven stations in or near the North Fork American, East Fork Carson, and Merced River basins (Figure 2) in the Sierra Nevada as dependent variables. The specific predictands for which regression models were fitted are the daily series of wet-day occurrence (O), wet-day amounts (R), and maximum (TMAX) and minimum (TMIN) temperatures. Regression relations were fitted on daily variables for the 10 years from 1979 to 1988 and were evaluated using the 7 years from 1989 to 1995. Separate regressions were undertaken for each station and each of the climatological seasons, winter (DJF), spring (MAM), summer (JJA), and autumn (SON).

All daily predictor variables were normalised using period means and standard deviations (as advocated by Karl et al., 1990) to increase transferability to GCM simulations, which may have different means and standard deviations from observed fields. The three most powerful predictor variables were selected following a step-wise multiple linear regression analysis of the 15 candidate variables listed in Table 2. The chosen predictors were gridded values of daily specific humidity (SH), the zonal velocity component of the surface geostrophic wind (Us, hereafter referred to as U), and 500 hPa geopotential heights (H).
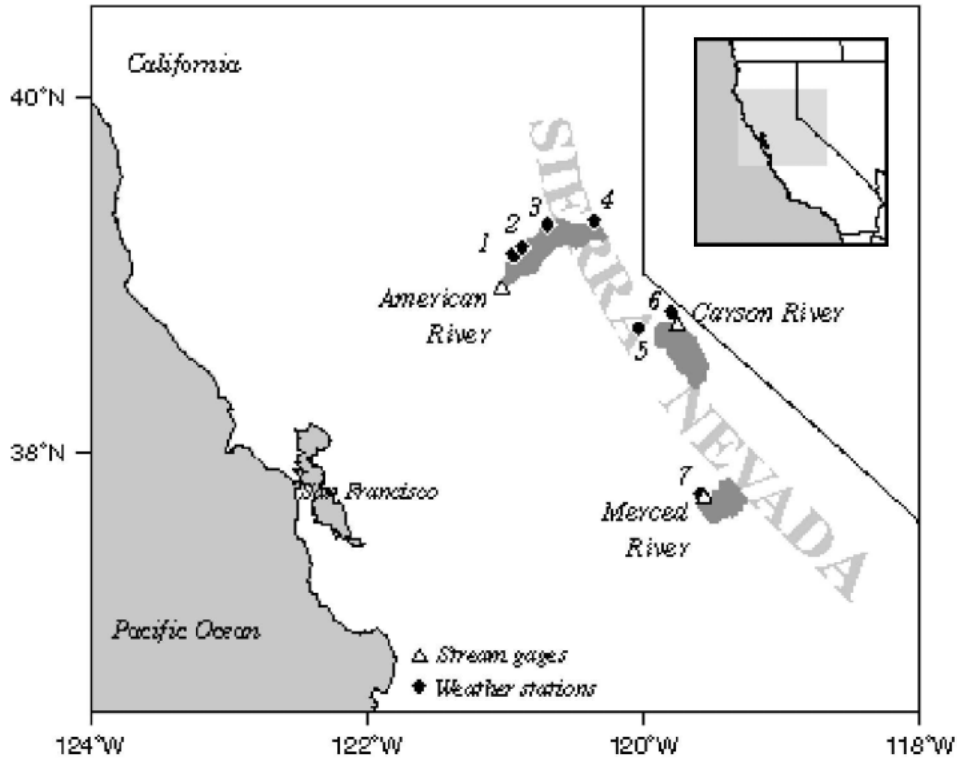
FIGURE 2. Locations of Sierra Nevada river basins, stream gauges, and meteorological stations; triangles indicate stream gauges at lowest points in shaded river basins, diamonds indicate weather stations used as inputs for the watershed models, at 1-Colfax, 2-Gold Run, 3-Blue Canyon, 4-Central Sierra Snow Laboratory, 5-Twin Lakes, 6-Woodfords, and 7-Yosemite National Park Headquarters.

3.2.1 Daily Precipitation Occurrence (O$_i$)

Daily values of a precipitation occurrence parameter O_i (represented by a series of "1"s and "0"s) were regressed against three grid-box predictor variables SH, U, H, and a lag-1 autocorrelation function using the following regression equation:

$$O_i = \alpha_0 + \alpha_{Oi-1}O_{i-1} + \alpha_{SH}SH_i + \alpha_U U_i + \alpha_H H_I \ . \tag{1}$$

The α parameters are fitted by using linear least squares regression. In simulation mode, a uniformly distributed random number r ($0 \leq r \leq 1$) is used to determine whether precipitation occurs. For a given site and day, a wet day is synthesized if $r \leq O_i$.

3.2.2 *Daily Precipitation Amounts (R$_i$)*

Wet-day precipitation amounts (R$_i$) for a given day *i* are downscaled using the three grid-box predictor variables *SH, U,* and *H*. Since R$_i$ is always non-zero, it is appropriate to formulate the following regression model (following Kilsby et al., 1998):

$$R_i = \exp(\beta_0 + \beta_{SH}SH_i + \beta_U U_i + \beta_H H_i + \varepsilon_i) \ , \tag{2}$$

where the β's are parameters fitted by linear least squares regression and ε_i is a random modelling error. The expected value is given by:

$$E(R_i) = \emptyset \ c_R \exp(\beta_0 + \beta_{SH}SH_i + \beta_U U_i + \beta_H H_i) \ , \tag{3}$$

where c_R is an empirically derived correction ratio that allows for the bias resulting from the re-transformation of $\ln(R)$ to R and the fact that ε_t comes from a skewed distribution. The value of c_R is defined such that observed and downscaled precipitation totals are equal for the calibration period. Additionally, a random scaling factor $\emptyset$ (with a mean of 1) is used to increase the variance of R to obtain better agreement with observations (as used by Hay et al., 1991). Note that a lag-1 autoregressive component is not used to model R$_i$ because its inclusion did not significantly improve the explained variance in wet-day amounts. However, it is acknowledged that this parameter may be appropriate at other locations.

3.2.3 *Daily Temperatures (TMAX$_i$ and TMIN$_i$)*

Daily maximum (*TMAX$_i$*) and minimum (*TMIN$_i$*) temperatures for a given day *i* were downscaled using the three grid-box predictor variables *SH, U,* and *H*, and the preceding day's maximum (*TMAX$_{i-1}$*) and minimum (*TMIN$_{i-1}$*) temperatures, respectively. The daily temperature series were modelled using the following regression equations:

$$TMAX_i = \delta_0 + \delta_{TMAXi-1}TMAX_{i-1} + \delta_{SH}SH_i + \delta_U U_i + \delta_H H_i + \zeta_i \tag{4}$$

and

$$TMIN_i = \gamma_0 + \gamma_{TMINi-1}TMIN_{i-1} + \gamma_{SH}SH_i + \gamma_U U_i + \gamma_H H_i + \xi_I \ , \tag{5}$$

where δ and γ are parameters fitted by linear least squares regression, and ζ_i and ξ_t are model errors. Both ζ_t and ξ_t are assumed to be normally distributed with mean zero and standard deviation σ equal to the standard error of the regression equation. Both sets of residuals were modelled stochastically using conventional Monte Carlo methods (Wilby et al., 1998a).

3.3 HYDROLOGICAL MODEL

The three river basins are simulated using parameterizations of daily heat and water budgets in the Precipitation-Runoff Modelling System (PRMS: Leavesley et al., 1983), a physically based, distributed parameter model of precipitation forms, snowpack evolution, and runoff generation. The spatial variability of land characteristics that affect snowpack and runoff is represented by hydrologic response units (HRUs), within which runoff responses to uniform precipitation or snowmelt inputs are assumed to be homogeneous. HRUs are characterized and delineated in terms of those physiographic properties that determine hydrologic responses: elevation, slope, aspect, vegetation, soils, geology, and climate (e.g., Smith and Reece, 1995). In the three models used here, HRUs were designed to incorporate all grid cells, on 100-m grids, that share nearly identical combinations of these seven physiographic properties, regardless of whether the grid cells in an HRU form a contiguous polygon (Jeton and Smith, 1993). The resulting "pixelated" model delineations represent the basins in terms of 50 HRUs in the American River model, 50 HRUs in the Carson River, and 64 HRUs in the Merced River.

Within each HRU, the heat- and water-budget responses to daily inputs of precipitation and daily fluctuations of air temperature are simulated. The daily mixes of rain and snow are estimated from each day's temperatures by interpolations between the temperatures at which precipitation historically has been either all snow or all rain (Willen et al., 1971). Interception losses, sublimation, and evapotranspiration are also parameterized and simulated in terms of precipitation and daily maximum and minimum temperatures. Runoff is partitioned between surface runoff, shallow-subsurface runoff, deep-subsurface runoff, and deep ground-water recharge on the basis of the simulated accumulations of soil moisture at each HRU and of water in deeper subsurface reservoirs that underlie multiple HRUs. The various processes acting on runoff generation from the basins are represented in sufficient detail that heat- and moisture-fluxes vary realistically with short- and long-term climatic variations. However, the particular model parameters (such as temperature thresholds for rain to fall) and various land-surface descriptors (such as plant-canopy densities) were not modified in the future-climate simulations. Thus, the details of the model's temperature-based parameterizations are assumed, in the present study, to be unchanged under the future-climate scenarios. This simplification amounts to assumptions that precipitation would derive from the same heights in the atmosphere as at present and that land-surface properties, such as vegetation type, would not change under the future scenarios.

Snowpack accumulation, evolution, and ultimately the heat and water balances of the snowmelt periods are critical components in the simulations and are driven by the daily inputs of precipitation and daily air temperatures (using the parameterizations of Obled and Rosse, 1977). Snowmelt in the Sierra Nevada is driven mostly by solar radiation rather than by direct inputs of heat from the surface-air temperatures (Aguado, 1985). Thus, the temperature-based parameterizations of daily solar-radiation inputs are an important component of the models. The method used is a simple correction of clear-sky insolation estimates – from latitude, HRU slope and aspect, and day of the year – using the occurrence of precipitation and daily maximum air temperatures as crude indicators of the presence or absence of cloud cover (see Leavesley et al., 1983). Heat deposited in

the snowpack by each day's sunshine is either lost to the overlying atmosphere the following evening if air temperatures drop below freezing, or is stored to contribute to eventual snowmelt if evening temperatures remain warmer than freezing.

These temperature-based snowpack and insolation parameterizations are assumed to be unchanged in the future-climate conditions. Because of the physical detail of the process representations in the models, this assumption is a reasonable simplification. In the models, however, the solar-radiation estimates are functionally tied to daily air temperatures. This means that simulated solar-radiation inputs increase along with air temperatures, and thus, in addition to being warmer and wetter, the future-climate condition is represented in the hydrological models – almost inadvertently – as also being less cloudy (on dry days) than the present condition. As more information describing future relations between daily temperatures, cloudiness, and solar radiation at the surface becomes available, the parameterization of solar-radiation inputs used in simulations of future climate conditions may need to be modified accordingly. In this study, the parameterization was the same in all simulations.

The Carson and American River models are described in detail by Jeton et al. (1996). The Carson River model simulates historical streamflows from 1969 to 1998, and the American River model simulates streamflow from 1949 to 1998. These simulations are driven by precipitation and temperature records from two nearby weather stations in the Carson River model and by weather observations from four nearby stations in the American River model. Indications of the goodness-of-fit of these models are presented by Jeton et al. (1996), and overall the fits are satisfactory. For example, 97 percent of the observed fluctuations of annual flow totals in the American River during a validation (non-calibration) period from 1949 to 1968 are present in the simulations, and 80 percent of the annual flow fluctuations of the Carson River are present in simulations during its validation period from 1969 to 1979. The Merced River model was designed to simulate daily flows for the period from 1916 to present (Dettinger et al., 1999), and the model is driven by precipitation and temperature observations from two long-term weather stations in the Sierra Nevada for most of that time (prior to the mid 1930s, only one of the two stations had weather records and the model was driven with just one input station). From 1937 to 1996, the model captures 77 percent of the observed daily flow variability; during the same period, simulated annual flow totals capture 83 percent of the observed variations.

4. Modelled Streamflow Under Current-Climate Conditions

The calibrated downscaling model was forced using normalized Reanalysis *SH, U.* and *H* predictor variables for the verification period 1989-95. Statistically downscaled series of daily PRCP, TMAX and TMIN at the seven stations then were used to drive the watershed models.

The downscaling model, as shown in Figure 3, captures the timing of the July precipitation minimum but underestimates the magnitude of the March maximum. Overall, the model has a slight dry bias (<3% error), yielding an annual precipitation total of 1117 mm instead of the observed 1143 mm. The downscaling model has a warm bias during November through January and a cold bias in February (Figures 3b and 3c). On

average, both the downscaled maximum and minimum temperatures are +0.2°C warmer than observed data (16.6 and 3.0°C instead of 16.4 and 2.8°C, respectively).
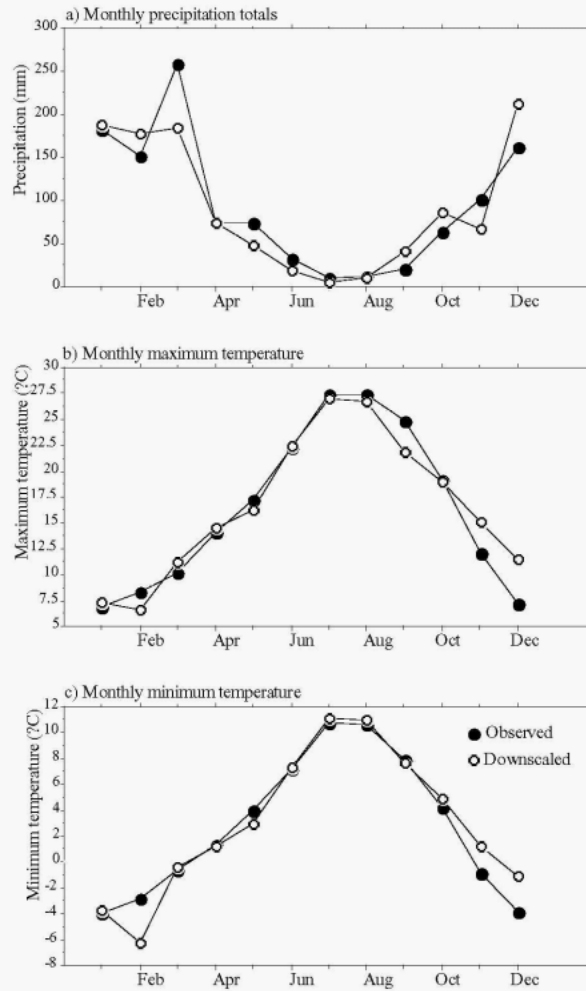

FIGURE 3. Observed and downscaled surface climate variables for the verification period 1989-95. Note that all seven stations were combined to produce the monthly means.

The success of the combination of hydrological models with precipitation and temperature downscaling can be measured in terms of biases in the simulated streamflow. The hydrological simulations driven by downscaled meteorology (Figure 4) generally underestimated annual streamflow, whereas simulations driven by station observations of meteorology tended to overestimate observed flows. Flows simulated using downscaled

meteorology averaged 90% of observed flows in the Merced, 93% in the Carson, and 92% in the American, in comparison with 106% for all station data.

Despite differences in simulated gross yields, the downscaled data provide a good approximation of the seasonal streamflow regimes, most notably for the Merced. However, the month of maximum mean streamflow is too early and too low in the case of the Carson, and well timed but underestimated in the American.
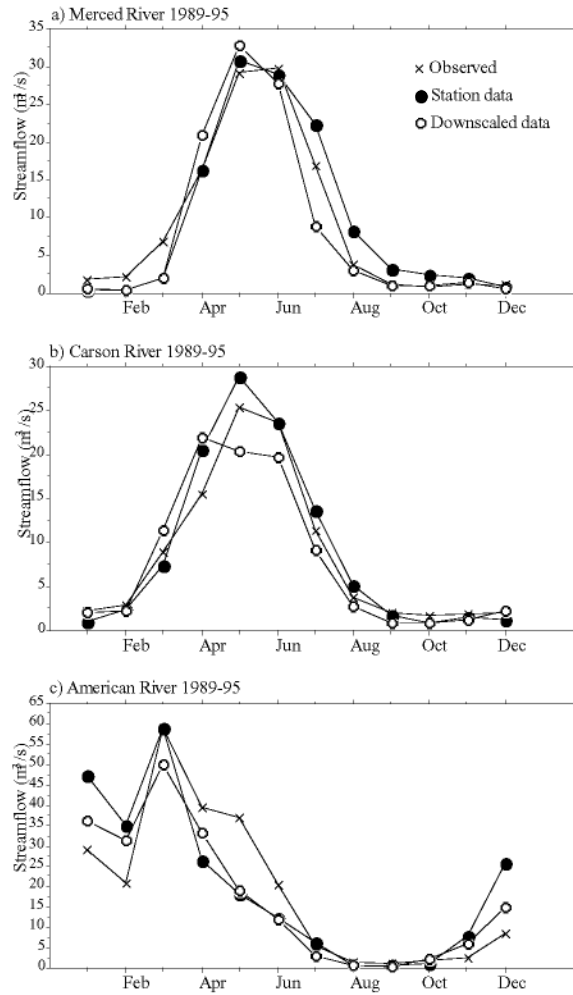

FIGURE 4. Monthly mean streamflow in the Merced, Carson, and American Rivers, 1989-95, simulated using station and downscaled data compared with gauged flows.
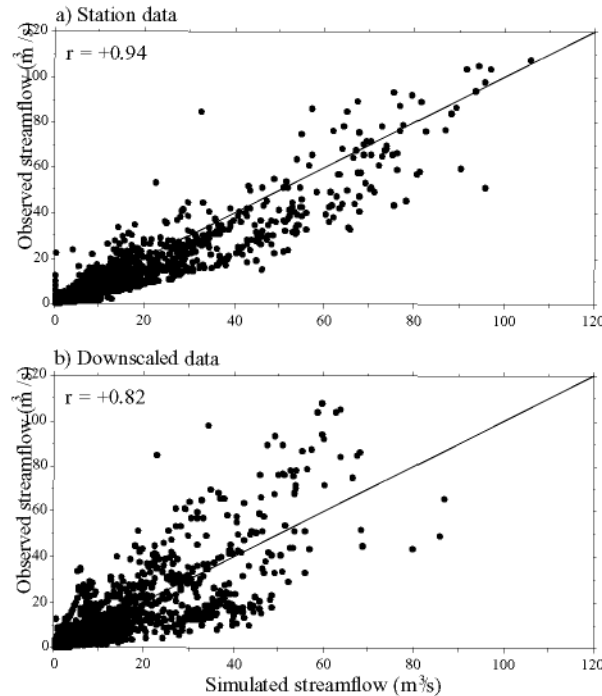
FIGURE 5. A comparison of observed and simulated daily streamflows
in the Carson River, 1989-95, using (a) station data, and (b) downscaled data.

A more severe test of the combined hydrological-downscaling model performance is provided by analysis of simulated daily flows for the downscaling-validation period from 1989 to 1995. As shown in Figure 5, for example, simulations forced by the station data have greater skill on daily time scales than do simulations with the downscaled meteorology for the Carson River model. For both simulations, though, the fits are satisfactory, and a significant component of the overall bias can be attributed to the hydrological model and choice of stations used for model calibration. Similarly, the correlation skills of flows simulated using statistically downscaled (station) data in the Merced and American Rivers were $r = +0.84$ (0.89) and $r = +0.67$ (0.81), respectively.

5. Modelled Streamflow Under Future-Climate Conditions

Having demonstrated the ability of the combination of the downscaled historical climate conditions with the hydrological models to reproduce realistic historical streamflow variations, we next simulated streamflow using downscaled GCM simulations. The downscaling model – as calibrated with the historical Reanalysis fields – was forced using daily SH, U, and H predictors simulated by HadCM2 for current (1980-99) and future (2080-99) climate conditions. The seasonal regimes of the surface variables downscaled from the two HadCM2 scenarios are shown in Figure 6, and the

corresponding streamflow and snowpack changes simulated by PRMS are shown in Figure 7.

The downscaled scenarios yield more than a 50% increase in the annual precipitation and a +3°C warming of maximum and minimum daily temperatures. However, indicated in Figure 6a, the bulk of the precipitation increase occurs in just three months; precipitation in December, January, and February increases by +104%. The increases in maximum temperature (Figure 6b) range from +5.6°C (September) to +1.6°C (February),
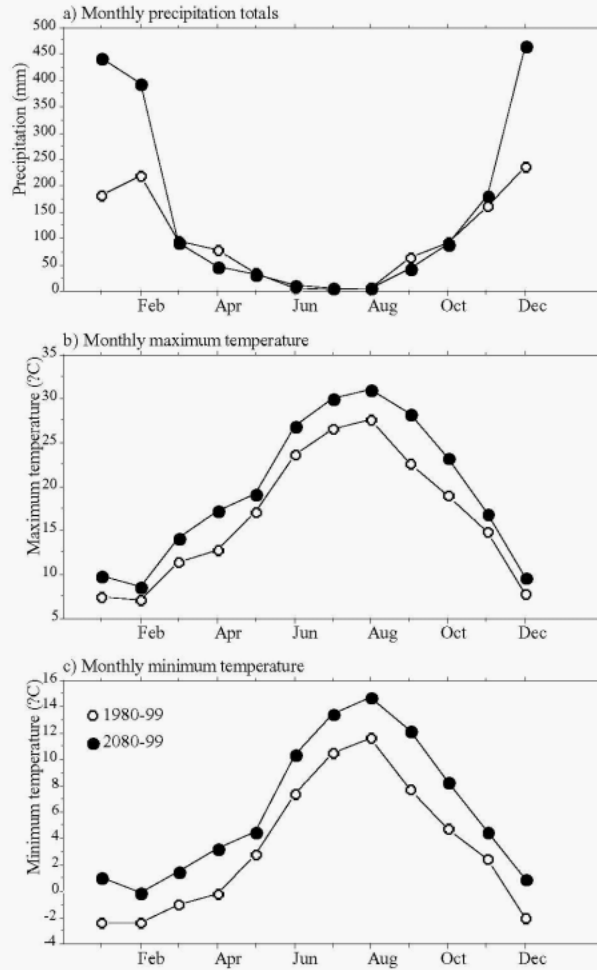

FIGURE 6. Downscaled surface climate variables produced using HadCM2 predictor variables under current (1980-99) and future (2080-99) climate conditions.

in comparison with +4.5°C (September) and +1.7°C (May) for the minimum temperatures (Figure 6c).

These changes in future precipitation and temperature regimes are reflected in simulated snowpack and streamflow changes (Figure 7). In response to increased precipitation totals, all three rivers show large increases in annual runoff, ranging from +107% in the Merced, through +103% in the Carson, to +82% in the American. The corresponding annual mean snowpack changes were +41% (Merced), +27% (Carson), and –6% (American). The Merced has the largest increase in winter snowpack with an earlier peak snow water content, and an increase that persists into the summer months. Increased snowpack is accompanied by a marked increase in Merced spring streamflows. Similar, but smaller, increases are simulated for the Carson River. Both of these rivers are mostly at high elevations and have cold winters and springs. Evidently, the warmer temperatures in the simulated future-climate conditions are not sufficiently warm to prevent significant increases in overall snowpack and springtime streamflow. Indeed, in spite of projected warmer conditions, the percentage of the Merced and Carson basins that is simulated as being snowcovered – on average – during December through March decreases by only about 5% of current snow-covered areas. Thus, although warmer temperatures would tend to reduce the snow-covered areas, much wetter winter conditions roughly compensate for the reduced snow-covered areas in these simulations.
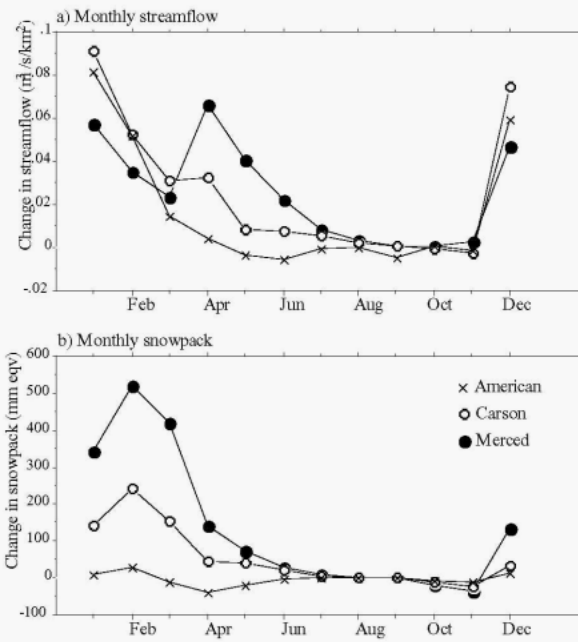

FIGURE 7. Changes in specific streamflow (streamflow divided by basin area) and snowpack (water-equivalent depths) between 1980-99 and 2080-99.

In contrast, simulations of the American River indicate only a slight increase in winter snowpack and a decrease in spring snowpack volumes. Snow-covered areas in the American River basin decrease by about 10% of current averages under the warmer and wetter future-climate scenario. The American River basin is lower and warmer than the others, and it yields a mix of rainfall runoff and snowmelt runoff each year, under current conditions. Increased winter streamflows projected under future-climate conditions are due to increases in winter rainfall runoff rather than increased snowmelt runoff. This results in earlier peak streamflows for the American and Carson Rivers under future climate conditions. All three basins yield more cool-season flash flooding under the future-climate conditions, and all have less autumn snowpack owing to higher maximum and minimum temperatures in September and a slight decrease in autumn precipitation.

6. Discussion

A recent synthesis of seasonal precipitation scenarios for North America predicted by 15 GCMs reported changes ranging from –4% to +8% per 1°C global-mean warming, with wintertime precipitation over California being the most sensitive season and region (Wigley, 1999). Particular models such as CGCM1 and HadCM2 (Figure 1) simulate even greater sensitivities. For example, changes in the winter precipitation of HadCM2 range from –10%/°C over southern Texas to +20%/°C over California. Although such results may be useful for identifying regions that are potentially most vulnerable to climate variability and change, GCMs are unable to capture local climatic effects arising from topographic, coastal, and land-surface processes. Statistical downscaling offers a computationally efficient and robust method of generating the basin-scale climate-change estimates necessary for hydrological impact assessments.

Accordingly, a regression-based downscaling method was used to simulate daily rainfall and temperature series for streamflow modelling in three Californian river basins under current- and future-climate conditions. The downscaling model employed just three predictor variables (specific humidity, zonal velocity component of airflow, and 500 hPa geopotential heights) supplied by HadCM2 for the grid point nearest the target basins. When evaluated using independent data, the model showed reasonable skill at reproducing observed area-average precipitation, temperature, and concomitant streamflow variations. Overall, the downscaled data resulted in slight underestimates of mean annual streamflow that can be attributed to underestimates of precipitation in spring and positive temperature biases in winter.

Simulated streamflows provide a useful indication of the combined skill of the coupled downscaling-hydrological model for the current climate because streamflow is an effective integrator (in time and space) of the cumulative effects of multiple climate variables. Streamflow at a single gaging site can also be measured more reliably than areal-average precipitation or temperature in complex terrain. However, because rivers act as basin-scale and season-long integrators of climatic forcings, simple downscaling-skill measures applied to streamflow simulations can appear more skillful than would similar skill measures applied to the driving precipitation and temperature inputs. For example, in basins with significant snowpack, the gross accumulations of precipitation in the seasonal snowpack and the timing of spring melt are critical to the simulations of hydrological responses. Conversely, in rainfall-dominated basins, the timing and

magnitude of individual storm events are of greater concern, and these individual storms are the most difficult for a downscaling model to reproduce given only synoptic-scale atmospheric-circulation inputs. Thus, if a downscaling method reproduces only seasonal totals of precipitation and realistic temperature fluctuations during the critical snowmelt periods, snowmelt-dominated rivers will be much better represented than will nearby rivers dominated by rainfall runoff. Even in a rainfall-driven system, though, soil-moisture and ground-water reservoirs will tend to smooth the hydrological response and contribute apparent skill to the downscaling

The smoothing effects of snowpack on streamflow responses to climate forcings help to explain differences between the skill of simulated streamflows in the three basins. The Merced and American River basins drain the western, windward slope of the Sierra Nevada, whereas the Carson River drains the eastern, leeward slope. Hence, the Carson River basin is in the rain shadow of the Sierra Nevada and is drier than the others. The Merced and Carson River basins are high-elevation basins and cool overall, with the part of the Merced drainage simulated here ranging from 1,200 to over 4,000 m above sea level and the Carson River drainage ranging from 1,600 to 3,400 m. The American River basin is a lower elevation basin and warmer overall, ranging from 200 m to 2,500 m above sea level. Consequently, the Merced and Carson Rivers are snowmelt dominated whereas the American River is a mix of rainfall runoff and snowmelt runoff. Simulated streamflow in the American River responds rapidly and sensitively to daily-scale temperature and precipitation fluctuations and errors; in the Merced and Carson Rivers, the response to the same short-term influences is much less. Consequently, the skill of simulated flows was significantly lower in the American River model than in the Carson and Merced.

The physiography of the three basins also accounts for differences in their sensitivities to future climate change. Increases in winter precipitation exceeding +100% coupled with mean temperature rises greater than +2°C result in increased winter streamflows in all three basins. In the Merced and Carson basins, these streamflow increases reflect large changes in winter snowpack, whereas the streamflow changes in the lower elevation American basin are driven primarily by rainfall runoff. Furthermore, reductions in winter snowpack in the American River basin, owing to less precipitation falling as snow and earlier melting of snow at middle elevations, lead to less spring and summer streamflow.

Taken collectively, the downscaling results imply significant changes to both the timing and magnitude of streamflows in the Sierra Nevada by the end of the 21st Century. In the higher elevation basins, the HadCM2 scenario implies more annual streamflow and more streamflow during the spring and summer months, which are critical for water-resources management in California. Not shown here, but of comparable concern, the future winter and spring flow simulations also include more sudden flood events in response to winter and spring storms that yield more rainy mixes of rain and snow than at present, and for that rain to fall on snowpacks that are warmer than at present. Nearly all of the additional flow in the lower elevation, warmer American River basin occurs in winter and constitutes increased flood hazards. Thus, depending on the relative significance of rainfall runoff and snowmelt, each basin responds in its own way to regional climate forcing. Generally, then, climate scenarios need to be specified—by whatever means—with sufficient temporal and spatial resolution to capture subtle

orographic influences if projections of climate-change responses are to be useful and reproducible.

7. Acknowledgments

8. References

Aguado, E. 1985. Radiation balances of melting snow covers at an open site in the central Sierra Nevada, California. *Water Resources Research*, **21**, 1649-1654.

Bardossy, A. and Plate, E.J. 1992. Space-time model for daily rainfall using atmospheric circulation patterns. *Water Resources Research*, **28**, 1247-1259.

Boer, G.J., Flato, G.M. and Ramsden, D. 1999a. A transient climate change simulation with historical and projected greenhouse gas and aerosol forcing: projected climate for the 21st century. *Climate Dynamics*, submitted.

Boer, G.J., Flato, G.M., Reader, M.C. and Ramsden, D. 1999b. A transient climate change simulation with historical and projected greenhouse gas and aerosol forcing: experimental design and comparison with the instrumental record for the 20th century. *Climate Dynamics*, submitted.

Christensen, J.H., Machenhauer, B., Jones, R.G., Schär, C., Ruti, P.M., Castro, M., Visconti, G. 1997. Validation of present-day regional climate simulations over Europe: LAM simulations with observed boundary conditions. *Climate Dynamics*, **13**, 489-506.

Conway, D., Wilby, R.L. and Jones, P.D. 1996. Precipitation and air flow indices over the British Isles. *Climate Research*, **7**, 169-183.

Crane, R.G. and Hewitson, B.C. 1998. Doubled CO2 precipitation changes for the Susquehanna basin: downscaling from the GENESIS General Circulation Model. *International Journal of Climatology*, **18**, 65-76.

Dettinger, M.D., and Cayan, D.R., 1992, Climate-change scenarios for the Sierra Nevada, California, based on winter atmospheric-circulation patterns: Proceedings, 1992 American Water Resources Association Symposium and Conference, "Managing Water Resources under Global Change," Reno, Nevada, 681-690.

Dettinger, M.D., Mo, K., Cayan, D.R., and Jeton, A.E. 1999. Global to local scale simulations of streamflow in the Merced, American, and Carson Rivers, Sierra Nevada, California: Preprints, *American Meteorological Society's 14th Conference on Hydrology*, Dallas, January 1999, 80-82.

Felzer, B. 1999. Hydrological implications of GCM results for the U.S. National Assessment. *Proceedings of the Speciality Conference on Potential Consequences of Climate Variability and Change to Water Resources of the United States*, American Water Resources Association, Atlanta, USA, 69-72.

Flato, G.M., Boer, G.J., Lee, W.G., McFarlane, N.A., Ramsden, D., Reader, M.C. and Weaver, A.J. 1999. The Canadian Centre for Climate Modelling and Analysis Global Coupled Model and its climate. *Climate Dynamics*, submitted.

Giorgi, F. and Mearns, L.O. 1991. Approaches to the simulation of regional climate change. A review. *Rev. Geophys.*, **29**, 191-216.

Giorgi, F. and Mearns, L.O. 1999. Introduction to special section: Regional climate modelling revisited. *Journal of Geophysical Research*, **104**, 6335-6352.

Goodess, C.M. and Palutikof, J.P. 1998. Development of daily rainfall scenarios for southeast Spain using a circulation-type approach to downscaling. *International Journal of Climatology*, **10**, 1051-1083.

Gregory, J.M., Wigley, T.M.L. and Jones, P.D. 1993. Application of Markov models to area-average daily precipitation series and interannual variability in seasonal totals. *Climate Dynamics*, **8**, 299-310.

Hay, L.E., McCabe, G.J., Wolock, D.M. and Ayers, M.A. 1991. Simulation of precipitation by weather type analysis. *Water Resources Research*, **27**, 493-501.

Hay, L.E., McCabe, G.J., Wolock, D.M. and Ayers, M.A. 1992. Use of weather types to disaggregate General Circulation Model predictions. *Journal of Geophysical Research*, **97**, 2781-2790.

Hostetler, S.W. 1994. Hydrologic and atmospheric models: the (continuing) problem of discordant scales. *Climatic Change*, **27**, 345-350.

Jeton, A.E. and Smith, J.L. 1993. Development of watershed models for two Sierra Nevada basins using a geographic information system. *Water Resources Bulletin*, **29**, 923-932.

Jeton, A.E. Dettinger, M.D., and Smith, J.L. 1996. Potential effects of climate change on streamflow, eastern and western slopes of the Sierra Nevada, California and Nevada. *U.S. Geological Survey Water-Resources Investigations Report* 95-4260, 44 p.

Johns, T.C., Carnell, R.E., Crossley, J.F., Gregory, J.M., Mitchell, J.F.B., Senior, C.A., Tett, S.F.B. and Wood, R.A. 1997. The Second Hadley Centre coupled ocean-atmosphere GCM: Model description, spinup and validation. *Climate Dynamics*, **13**, 103-134.

Jones, P.D., Hulme, M. and Briffa, K.R. 1993. A comparison of Lamb Circulation Types with an objective classification scheme. *International Journal of Climatology*, **13**, 655-663.

Jones, R.G., Murphy, J.M. and Noguer, M. 1995. Simulation of climate change over Europe using a nested regional-climate model. I: Assessment of control climate, including sensitivity to location of lateral boundaries. *J. Roy. Met. Soc.*, **121**, 1413-1449.

Kalnay, E., Kanamitsu, M., Kistler, R., Collins, W., Deaven, D., Gandin, L., Iredell, M., Saha, S., White, G., Woollen, J., Zhu, Y., Chelliah, M., Ebisuzaki, W., Higgins, W., Janowiak, J., Mo, K.C., Ropelewski, C., Wang, J., Leetmaa, A., Reynolds, R., Jenne, R. and Joseph, D. 1996. The NCEP/NCAR 40-year reanalysis project. *Bulletin of the American Meteorological Society*, **77**, 437-471.

Karl, T.R., Wang, W.C., Schlesinger, M.E., Knight, R.W. and Portman, D. 1990. A method of relating General Circulation Model simulated climate to the observed local climate. Part I: Seasonal statistics. *Journal of Climate*, **3**, 1053-1079.

Katz, R.W. 1996. Use of conditional stochastic models to generate climate change scenarios. *Climatic Change*, **32**, 237-255.

Kilsby, C.G., Cowpertwait, P.S.P., O'Connell, P.E. and Jones, P.D. 1998. Predicting rainfall statistics in England and Wales using atmospheric circulation variables. *International Journal of Climatology*, **18**, 523-539.

Leavesley, G.H., Lichty, R.W., Troutman, B.M. and Saindon, L.G. 1983. Precipitation-runoff modelling system: User's manual. *U.S. Geological Survey Water-Resources Investigations Report* 83-4238, 207 p.

Matyasovszky, I., Bogardi, I. And Duckstein, L. 1994. Comparison of two GCMs to downscale local precipitation and temperature. *Water Resources Research*, **30**, 3437-3448.

McGregor, J.J. 1997. Regional climate modelling. *Meteorol. Atmos. Phys.*, **63**, 105-117.

Mearns, L.O., Rosenzweig, C. and Goldberg, R. 1996. The effect of changes in daily and interannual climatic variability on CERES-wheat yields. A sensitivity study. *Climatic Change*, **32**, 257-292.

Mitchell, J.F.B. and Johns, T.C. 1997. On modification of global warming by sulphate aerosols. *Journal of Climate*, **10**, 245-267.

Obled, C. and Rosse, B.B. 1977. Mathematical models of a melting snowpack at an index plot. *J. Hydrology*, **32**, 139-163.

Pilling, C., Wilby, R.L. and Jones, J.A.A. 1998. Downscaling of catchment hydrometeorology from GCM output using airflow indices in upland Wales. In: Wheater, H. and Kirby, C. *Hydrology in a Changing Environment*, Vol.1, Wiley, Chichester, 191-208.

Richards, J.M. 1971. Simple expression for the saturation vapour pressure of water in the range -50° to 140°. *Brit. J., Appl. Phys.*, **4**, L15-L18.

Richardson, C.W. 1981. Stochastic simulation of daily precipitation, temperature and solar radiation. *Water Resources Research*, **17**, 182-190.

Smith, J.L. and Reece, B.D. 1995. Watershed characterization for precipitation runoff modelling system, North Fork American River and East Fork Carson River watersheds, California. *U.S. Geological Survey Hydrologic Investigations Atlas* HA-734, 1 sheet.

von Storch, H., Zorita, E. and Cubasch, U. 1993. Downscaling of global climate change estimates to regional scales: an application to Iberian rainfall in wintertime. *J. Climate*, **6**, 1161-1171.

Wigley, T.M.L. 1999. *The science of climate change: global and U.S. perspectives*. Pew Center on Global Climate Change, Arlington, Virginia, 48 pp.

Wilby, R.L. 1997. Nonstationarity in daily precipitation series: implications for GCM downscaling using atmospheric circulation indices. *International Journal of Climatology*, **17**, 439-454.

Wilby, R.L. and Wigley, T.M.L. 1997. Downscaling General Circulation Model output: a review of methods and limitations. *Progress in Physical Geography*, **21**, 530-548.

Wilby, R.L., Hassan, H. and Hanaki, K. 1998a. Statistical downscaling of hydrometeorological variables using general circulation model output. *Journal of Hydrology*, **205**, 1-19.

Wilby, R.L., Wigley, T.M.L., Conway, D., Jones, P.D., Hewitson, B.C., Main, J., and Wilks, D.S. 1998b. Statistical downscaling of General Circulation Model output: a comparison of methods. *Water Resources Research*, **34**, 2995-3008.

Wilby, R.L., Hay, L.E. and Leavesley, G.H. 1999. A comparison of downscaled and raw GCM output: implications for climate change scenarios in the San Juan River basin, Colorado. *Journal of Hydrology*, submitted.

Wilks, D.S. 1992. Adapting stochastic weather generation algorithms for climate change studies. *Climatic Change*, **22**, 67-84.

Willen, D.W., Shumway, C.A., and Reid, J.E. 1971. Simulation of daily snow water equivalent and melt. *Proceedings of the 1971 Western Snow Conference*, Billings, Montana, v. 39, 1-8.

Winkler, J.A., Palutikof, J.P., Andresen, J.A. and Goodess, C.M. 1997. The simulation of daily temperature series from GCM output. Part II: Sensitivity analysis of an empirical transfer function methodology. *Journal of Climate*, **10**, 2514-2532.